JACS
JOURNAL OF THE AMERICAN CHEMICAL SOCIETY

Communication

pubs.acs.org/JACS

Discrete Stacking of Aromatic Oligoamide Macrocycles

Xiangxiang Wu,[†,∥,⊥] Rui Liu,[†,‡,⊥] Bharathwaj Sathyamoorthy,[‡] Kazuhiro Yamato,[‡] Guoxing Liang,[‡] Lin Shen,[‡] Sufang Ma,[†] Dinesh K. Sukumaran,[‡] Thomas Szyperski,[‡] Weihai Fang,[†] Lan He,*[,§] Xuebo Chen,*[,†] and Bing Gong*[,†,‡]

[†]Key Laboratory of Theoretical and Computational Photochemistry of the Ministry of Education, College of Chemistry, Beijing Normal University, Beijing 100875, China

[‡]Department of Chemistry, The State University of New York at Buffalo, Buffalo, New York 14260, United States

[§]National Institute for Food and Drug Control, Beijing 100050, China

Supporting Information

ABSTRACT: Unlike the precise structural control typical of closed assemblies, curbing the stacking of disc- and ring-shaped molecules is quite challenging. Here we report the discrete stacking of rigid aromatic oligoamide macrocycles **1**. With increasing concentration, the aggregation of **1** quickly plateaus, forming a discrete oligomer, as suggested by 1D ^{1}H, 2D nuclear Overhauser effect, and diffusion-ordered NMR spectroscopy. Quantum-chemical calculations indicate that the tetramer of **1** is the most stable among oligomeric stacks. X-ray crystallography revealed a tetrameric stack containing identical molecules adopting two different conformations. With a defined length and an inner pore capable of accommodating distinctly different guests, the tetramers of **1** densely pack into 2D layers. Besides being a rare system of conformation-regulated supramolecular oligomerization, the discrete stacks of **1**, along with their higher-order assemblies, may offer new nanotechnological applications.

Among known nanotubular structures, organic nanotubes have unique advantages,[1] and the stacking of ring-shaped building blocks offers a conceptually straightforward approach for constructing such nanotubes.[1a,b,d,2] Aside from their fascinating properties, tubular stacks consisting of defined numbers of building blocks, or discrete nanotubes, may help elucidate the factors responsible for aligning ring-shaped molecules, leading to a much-needed correlation between different structural levels. However, the stacking of flat aromatic[3] or ring-shaped[1a,b,d,2] molecules almost invariably leads to extended stacks. Unlike the spontaneous formation and precise dimensional control of closed assemblies,[4] curbing the stacking of disclike molecules or assemblies usually relies on templation or tethering,[5] chain-stopping,[6] or the introduction of anticooperative interactions.[7] To date, few examples of discrete tubular assemblies consisting of identical ring-shaped molecules are known.

Here we report the discrete stacking of macrocycles **1**. Initially designed to stack into extended tubular assemblies reinforced by side-chain H-bonding interactions, macrocycles **1** exhibited only insignificant aggregation,[8] which was in sharp contrast to the strong association of analogous macrocycles.[9] The current study indicates that macrocycles **1**, instead of forming extended stacks, associate into dicrete stacks in solution and the solid state. Crystal structures of **1** reveal tubular stacks having a defined length and an inner pore with a fixed diameter defined by the constituent molecules. The self-assembling nanopore remains intact in the presence of different guests. The discrete stacks of **1** closely pack into two-dimensional (2D) layers that further stack. To the best of our knowledge, the template-free tetramerization shown by **1** is unprecedented for the stacking of identical ring-shaped molecules. Such supramolecular oligomerization of macrocycles is remarkable since most known ring-shaped molecules associate into polydisperse oligomeric or polymeric aggregates.

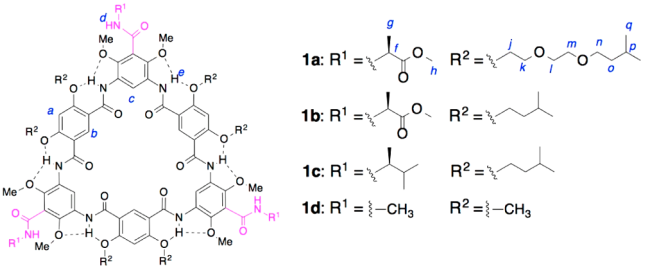

The ^{1}H NMR spectra of **1a** measured in $CDCl_3$ show that with increasing concentration the signals of amide protons *d* and *e* shift downfield initially and start to plateau beyond 20 mM and 10 mM, respectively (Figure S2a in the Supporting Information (SI)). Although the shift of protons *d* may be explained by H-bonding interactions, that of protons *e* cannot be, as protons *e* are engaged in highly favorable intramolecular three-center H-bonds[10] and cannot undertake additional H-bonding.[10a] The concentration-dependent shifts of protons *d* and *e* indicate that the self-association of **1a** similarly influences these protons located in different environments. This judgment is corroborated by the shifts of protons *a*, *b*, and *c*, which are incapable of H-bonding but nevertheless show an initial shift followed by a plateau region as the concentration of **1a** increases (Figure S2b). At elevated concentrations, the plateauing of the shifts and the well-dispersed ^{1}H NMR signals imply that further aggregation of **1a** is being curbed.

Received: March 12, 2015
Published: April 24, 2015

DOI: 10.1021/jacs.5b02552
J. Am. Chem. Soc. 2015, 137, 5879−5882

The aggregation of **1a** was confirmed by ^{1}H diffusion-ordered NMR spectroscopy (DOSY). At 9 °C, the apparent translational diffusion coefficient (D) of **1a** increased with decreasing concentration (Figure 1), indicating reduced aggregation of **1a** with decreasing concentration. The same change in diffusion rate was observed at 25 °C (Figure S3).

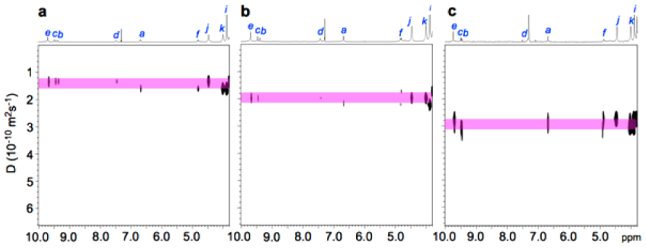

Figure 1. DOSY spectra of **1a** recorded at 9 °C in $CDCl_3$ at (a) 36, (b) 15, and (c) 1 mM. The values of D are based on the signals of protons *a*, *b*, *c*, *d*, *e*, *f*, *i*, *j*, and *k*.

The aggregation of **1a** was examined by estimating the apparent hydrodynamic volumes of **1a** in $CDCl_3$ relative to nonaggregating tetramethylsilane (TMS).[11] The ratios R_{1a}/R_{TMS}, where R_{1a} and R_{TMS} are the hydrodynamic radii of **1a** or its aggregates and TMS, respectively, were obtained from the measured diffusion coefficients D_{1a} and D_{TMS} (see the SI; $(R_{1a}/R_{TMS})^3$ equals V_{1a}/V_{TMS}, the ratio of hydrodynamic volumes). Concentration-dependent variations of V_{1a}/V_{TMS} reflect the extent of aggregation of **1a**. Importantly, using TMS as an internal reference eliminates contributions from varying solution viscosity,[11] which may change significantly as a function of the concentration of **1a**.

The apparent diffusion coefficients D_{1a} and D_{TMS} were measured in $CDCl_3$ at 9 °C (Table S1 in the SI). Increasing the concentration of **1a** retards the diffusion of **1a** and TMS differently. In going from 1 to 15 mM **1a**, D_{TMS} shows an insignificant change while D_{1a} decreases noticeably, suggesting that the slower diffusion of **1a** at 15 mM is mainly due to aggregation. As the concentration of **1a** further increases, the diffusion of TMS also slows down, indicating that the solution has become more viscous, while the diffusion of **1a** shows a much steeper slowdown, suggesting both a global change in viscosity and increased effective size due to self-association.

The values of $(R_{1a}/R_{TMS})^3$ at 15 and 36 mM are about 3- and 4-fold larger, respectively, than that at 1 mM (Table S1). If **1a** exists mainly as monomers at 1 mM, the 4-fold increase in the effective size observed at 36 mM, a concentration that lies beyond the "plateau region" where the ^{1}H signals show insignificant further shift (Figure S2), suggests that the macrocycles do not aggregate further and exist as discrete oligomers (i.e., tetramers) at this and higher concentrations. The values of $(R_{1a}/R_{TMS})^3$ measured at 25 °C are essentially the same as those obtained at 9 °C (Table S2), suggesting that the discrete aggregation of **1a** remains unchanged over this temperature range.

That single and precise apparent diffusion coefficients D_{1a} were measured for **1a** at 15 mM (Figures 1 and S3 and Tables S1 and S2), at which the monomeric and oligomeric species of **1a** have about the same abundance, suggests that the equilibrium between the monomeric and oligomeric species of **1a** must be very fast on the scale of the DOSY mixing time. Taken together with the manifestation of averaged ^{1}H NMR lines (Figure S2), this result indicates that the corresponding rate constants appear to be at least in the kilohertz range.

Examination of **1a** with 2D nuclear Overhauser effect spectroscopy (NOESY) revealed cross-peaks between the aromatic protons of the two different benzene residues at 36 mM but not at 1 mM (Figures S4–S9), suggesting that at elevated concentrations the macrocycles undergo well-aligned stacking involving their oligoamide backbones.

The limited aggregation of **1a** contrasts with the extended stacking typical of disc- or ring-shaped molecules. To gain additional insights, macrocycle **1d**, along with its oligomeric stacks, was examined computationally (see the SI). The semiempirical AM1 method[12] was used. Its reliability was verified by optimizing the monomer, dimer, and trimer of **1d** using density functional theory (DFT) with the M06 functional and the 6-31G* basis set (M06/6-31G*). The optimized structure of **1d** reveals planar and bowl-shaped conformations of similar stability (Figure S12), with the former being 0.9 and 1.8 kcal/mol more stable than the latter at the AM1 and M06/6-31G* levels, respectively. For the dimer of **2d**, only the one consisting of two planar macrocycles has an energy minimum (Figure S13), which is ∼4.0 and ∼5.0 kcal/mol less stable at the AM1 and M06/6-31G* levels, respectively, than two isolated planar molecules. The bond parameters of the two conformers of **1d** and those of the dimer and trimer optimized at both levels are very similar, indicating that the AM1 method reliably describes these structures.

Five oligomeric stacks of **1d** were energy-minimized at the AM1 level (Figure 2a). Unlike the dimeric stack, each of the

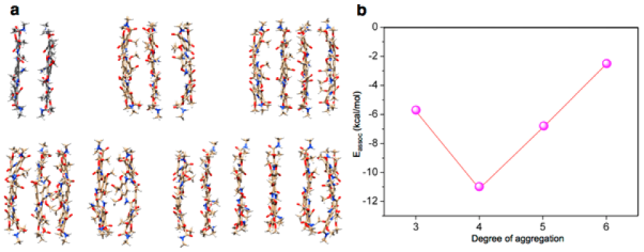

Figure 2. Optimized stacks of **1d**. (a) Side views of the dimeric, trimeric, tetrameric, pentameric, and hexameric stacks. (b) Plot of association energy vs degree of aggregation. The results are from optimizations at the AM1 level and were verified at the M06/6-31G* and M06/6-31G levels.

other four stacks has two end-capping bowl-shaped macrocyclic units and planar inner unit(s). The association energy (E_{assoc}) per macrocycle for each stack indicates that the tetramer, with $E_{assoc} \approx 11.0$ kcal/mol, is the most stable (Figure 2b). Optimizing the monomer, dimer, and trimer at the M06/6-31G* level and the tetramer and pentamer at the M06/6-31G level also indicates the tetramer to be the most stable ($E_{assoc} \approx$ 13.0 kcal/mol). Similar computations on **1c** showed its tetrameric stack to be the most stable (Figure S14). These results suggest that the tetramerization of **1** mainly depends on the macrocyclic backbone.

The tetramerization of **1** was confirmed by crystal structures. Single crystals of **1c** belong to the trigonal space group $R3$ ($a = b = 26.449$ Å, $c = 59.41$ Å, $\alpha = \beta = 90°$, and $\gamma = 120°$). Four molecules of **1c** stack into a discrete tube shaped like a quadruple-decker hamburger with a length of ∼18 Å and fixed inner and outer diameters of ∼8 and ∼26 Å, respectively (Figure 3a). This stack of **1c** consists of two planar "inner

DOI: 10.1021/jacs.5b02552
J. Am. Chem. Soc. 2015, 137, 5879–5882

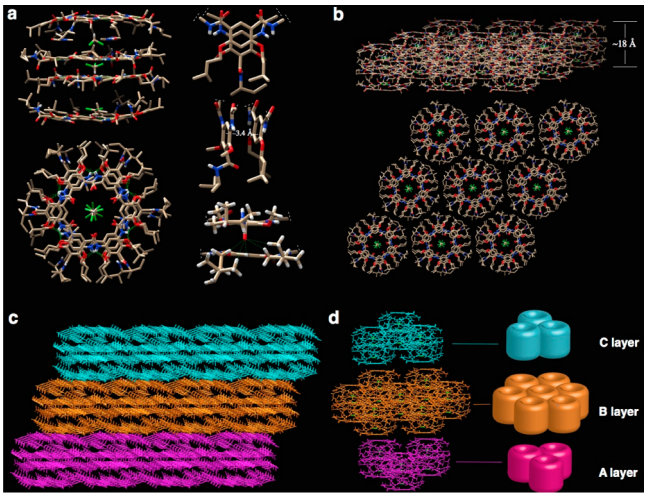

Figure 3. Crystal structure and further packing of the tetrameric stacks of **1c**. (a) Side and top views of the stack (left); the two different types of benzene residues of the inner cycles are at a close stacking distance (top and middle right); the side-chain amide oxygen from one of the inner cycles engages in numerous C−H···O-type contacts with the side-chain alkyl hydrogens of the other inner cycle (bottom right). All of the H atoms except those of NH groups have been removed for clarity. (b) Side and top views of the single layer consisting of hexagonally packed tetrameric stacks. (c) Side view of three stacked layers. (d) Exploded view of the vertical stacking of the 2D layers in the ...ABCABC... sequence. The cartoons show the orientation of each layer.

cycles" and two bowl-shaped "capping cycles" (Figure 3a, left). The inner cycles stack face-to-face, with one molecule rotated by 60° relative to the other, placing the two different types of benzene residues on top of each other (Figure 3a, top right). The inner cycles are located 3.4 Å apart (Figure 3a, middle right), indicative of strong $\pi-\pi$ stacking. In contrast, the two capping cycles are separated from the inner cycles by 7.0 and 6.7 Å, respectively. The capping and inner cycles exhibit numerous van der Waals contacts involving their side chains.

Surprisingly, none of the amide side chains of **1c** is involved in typical H-bonding interactions. The oxygen atoms of the side-chain amide groups of an inner cycle engage in multiple C−H···O contacts with the hydrogens of the isopentoxy side chains of the other inner cycle (Figure 3a, bottom right). Extended stacking of **1c** seems to be curbed by the bowl-like capping cycles, which place protruding electronegative amide oxygens on both ends of the tetrameric stack.

The tubular stacks of **1c** pack hexagonally into a layer with a thickness of ~18 Å and densely packed ~8 Å pores (Figure 3b). The 2D layers further stack by following the ...ABCABC... sequence of cubic closest packing observed for β-graphite[13] (Figure 3c). As a result, all of the nanotubular units along with their inner pores are oriented unidirectionally in the crystal structure (Figure 3d).

Although the crystal structure of **1b** could not be solved at high resolution, the diffraction data revealed unit cell parameters similar to those of **1c**: trigonal, $a = b = 27.29$ Å, $c = 72.28$ Å, $\alpha = \beta = 90°$, and $\gamma = 120°$.

The tubular stack of **1c** has an inner pore with a defined length (18 Å) and diameter (~8 Å) containing three chloroform molecules (Figure 3a). Three dimethylformamide molecules are sandwiched between the backbones of one of the capping cycles and its neighboring inner cycle.

The lumen of **1** was previously found to bind guanidinium ion.[8] Cocrystals of **1c** and guanidinium chloride (1:1) also belong to the trigonal $R3$ space group with unit cell parameters $a = b = 26.577$ Å, $c = 59.934$ Å, $\alpha = \beta = 90°$, and $\gamma = 120°$, which are nearly the same as those of **1c** alone. With four guanidinium ions in its inner pore, the tubular stack of **1c** remains unchanged, and these stacks pack hexagonally into layers that further stack in an ...ABCABC... sequence (Figure S11). Thus, replacing chloroform molecules with guanidinium ions in the inner pores does not compromise the integrity of the tetrameric stack and its 2D and 3D packing, which demonstrates the tenacity of this discrete tubular motif and its higher assemblies.

The stacking of **1** represents an unprecedented example of template-free, distinctly defined supramolecular oligomerization of ring-shaped molecules. The tubular stack of **1**, with a defined length and a fixed inner diameter, remains intact when accommodating suitable guests. Subsequent studies of this system may lead to a general strategy for controlling the stacking of ring-shaped molecules, leading to a variety of discrete self-assembling nanotubes. The hexagonal packing of the self-assembling nanotubes observed in single crystals result in a 2D layer consisting of densely packed subnanometer pores with a very high pore density (2×10^{13} pores/cm^2). Further stacking of the 2D layers leads to an organic framework with densely packed, uniformly oriented pores. The tubular stacks and the 2D and 3D frameworks provide a multilevel platform on the basis of which new functional materials and devices may be developed.

■ ASSOCIATED CONTENT

Ⓢ Supporting Information

Experimental conditions, NMR spectra, details of theoretical calculations and X-ray crystallography, and CIF files. The Supporting Information is available free of charge on the ACS Publications website at DOI: 10.1021/jacs.5b02552.

■ AUTHOR INFORMATION

Corresponding Authors

*bgong@buffalo.edu
*xuebochen@bnu.edu.cn
*helan1961@yahoo.com.cn

Present Address

‖X.W.: Henan University of Traditional Chinese Medicine, Zhengzhou, Henan, China, 450046.

Author Contributions

⊥X.W. and R.L. contributed equally.

Notes

The authors declare no competing financial interest.

■ ACKNOWLEDGMENTS

This work was supported by the National Natural Science Foundation of China (NSFC-91227109 and NSFC-21421003), the Major State Basic Research Development Program of China (2011CB808503), and the U.S. National Science Foundation (CHE-1306326, CBET-1066947, and MCB-0817857).

■ REFERENCES

(1) (a) Bong, D. T.; Clark, T. D.; Granja, J. R.; Ghadiri, M. R. *Angew. Chem., Int. Ed.* **2001**, *40*, 988. (b) Block, M. A. B.; Kaiser, C.; Khan, A.; Hecht, S. *Top. Curr. Chem.* **2005**, *245*, 89. (c) Sakai, N.; Mareda, J.;

DOI: 10.1021/jacs.5b02552
J. Am. Chem. Soc. 2015, 137, 5879−5882

Matile, S. *Acc. Chem. Res.* **2008**, *41*, 1354. (d) Gong, B.; Shao, Z. F. *Acc. Chem. Res.* **2013**, *46*, 2856.
(2) (a) Ghadiri, M. R.; Granja, J. R.; Milligan, R. A.; McRee, D. E.; Khazanovich, N. *Nature* **1993**, *366*, 324. (b) Seebach, D.; Matthews, J. L.; Meden, A.; Wessels, T.; Baerlocher, C.; McCusker, L. B. *Helv. Chim. Acta* **1997**, *80*, 173. (c) Gattuso, G.; Menzer, S.; Nepogodiev, S. A.; Stoddart, J. F.; Williams, D. J. *Angew. Chem., Int. Ed. Engl.* **1997**, *36*, 1451. (d) Mindyuk, O. Y.; Stetzer, M. R.; Heiney, P. A.; Nelson, J. C.; Moore, J. S. *Adv. Mater.* **1998**, *10*, 1363. (e) Fritzsche, M.; Bohle, A.; Dudenko, D.; Baumeister, U.; Sebastiani, D.; Richardt, G.; Spiess, H. W.; Hansen, M. R.; Höger, S. *Angew. Chem., Int. Ed.* **2011**, *50*, 3030. (f) Zhou, X. B.; Liu, G. D.; Yamato, K.; Shen, Y.; Cheng, R. X.; Wei, X. X.; Bai, W. L.; Gao, Y.; Li, H.; Liu, Y.; Liu, F. T.; Czajkowsky, D. M.; Wang, J. F.; Dabney, M. J.; Cai, Z. H.; Hu, J.; Bright, F. V.; He, L.; Zeng, X. C.; Shao, Z. F.; Gong, B. *Nat. Commun.* **2012**, *3*, 949. (g) Liu, Z. C.; Liu, G. L.; Wu, Y. L.; Cao, D.; Sun, J. L.; Schneebeli, S. T.; Nassar, M. S.; Mirkin, C. A.; Stoddart, J. F. *J. Am. Chem. Soc.* **2014**, *136*, 16651. (h) Hjelmgaard, T.; Roy, O.; Nauton, L.; El-Ghozzi, M.; Avignant, D.; Didierjean, C.; Taillefumier, C.; Faure, S. *Chem. Commun.* **2014**, *50*, 3564.
(3) (a) Adam, D.; Schuhmacher, P.; Simmerer, J.; Haussling, L.; Siemensmeyer, K.; Etzbach, K. H.; Ringsdorf, H.; Haarer, D. *Nature* **1994**, *371*, 141. (b) Engelkamp, H.; Middelbeek, S.; Nolte, R. J. M. *Science* **1999**, *284*, 785. (c) Hirschberg, J. H. K. K.; Brunsveld, L.; Ramzi, A.; Vekemans, J. A. J. M.; Sijbesma, R. P.; Meijer, E. W. *Nature* **2000**, *407*, 167.
(4) (a) Conn, M. M.; Rebek, J., Jr. *Chem. Rev.* **1997**, *97*, 1647. (b) Kolotuchin, S. V.; Zimmerman, S. C. *J. Am. Chem. Soc.* **1998**, *120*, 9092. (c) Meissner, R. S.; Rebek, J., Jr.; Demendoza, J. *Science* **1995**, *270*, 1485. (d) Takeda, N.; Umemoto, K.; Yamaguchi, K.; Fujita, M. *Nature* **1999**, *398*, 794. (e) Hasenknopf, B.; Lehn, J.-M.; Kneisel, B. O.; Baum, G.; Fenske, D. *Angew. Chem., Int. Ed. Engl.* **1996**, *35*, 1838. (f) Sessler, J. L.; Sathiosatham, M.; Doerr, K.; Lynch, V.; Abboud, K. A. *Angew. Chem., Int. Ed.* **2000**, *39*, 1300. (g) Atwood, J. L.; Barbour, L. J.; Jerga, A. *Proc. Natl. Acad. Sci. U.S.A.* **2002**, *99*, 4837. (h) Leigh, D. A.; Pritchard, R. G.; Stephens, A. J. *Nat. Chem.* **2014**, *6*, 978.
(5) (a) Lokey, R. S.; Iverson, B. L. *Nature* **1995**, *375*, 303. (b) Marlow, A. L.; Mezzina, E.; Spada, G. P.; Masiero, S.; Davis, J. T.; Gottarelli, G. *J. Org. Chem.* **1999**, *64*, 5116. (c) Klosterman, J. K.; Yamauchi, Y.; Fujita, M. *Chem. Soc. Rev.* **2009**, *38*, 1714. (d) Talukdar, P.; Bollot, G.; Mareda, J.; Sakai, N.; Matile, S. *J. Am. Chem. Soc.* **2005**, *127*, 6528. (e) Yoshizawa, M.; Nakagawa, J.; Kurnazawa, K.; Nagao, M.; Kawano, M.; Ozeki, T.; Fujita, M. *Angew. Chem., Int. Ed.* **2005**, *44*, 1810. (f) Gonzalez-Rodriguez, D.; van Dongen, J. L. J.; Lutz, M.; Spek, A. L.; Schenning, A. P. H. J.; Meijer, E. W. *Nat. Chem.* **2009**, *1*, 151. (g) Chen, Z. Z.; Urban, N. D.; Gao, Y.; Zhang, W. R.; Deng, J. G.; Zhu, J.; Zeng, X. C.; Gong, B. *Org. Lett.* **2011**, *13*, 4008. (h) Stojaković, J.; Whitis, A. M.; MacGillivray, L. R. *Angew. Chem., Int. Ed.* **2013**, *52*, 12127.
(6) Lortie, F.; Boileau, S. B.; Bouteiller, L.; Chassenieux, C.; Laupretre, F. *Macromolecules* **2005**, *38*, 5283.
(7) Besenius, P.; Portale, G.; Bomans, P. H. H.; Janssen, H. M.; Palmans, A. R. A.; Meijer, E. W. *Proc. Natl. Acad. Sci. U.S.A.* **2010**, *107*, 17888.
(8) Wu, X. X.; Liang, G. X.; Ji, G.; Fun, H. K.; He, L.; Gong, B. *Chem. Commun.* **2012**, *48*, 2228.
(9) (a) Yang, Y. A.; Feng, W.; Hu, J. C.; Zou, S. L.; Gao, R. Z.; Yamato, K.; Kline, M.; Cai, Z. H.; Gao, Y.; Wang, Y. B.; Li, Y. B.; Yang, Y. L.; Yuan, L. H.; Zeng, X. C.; Gong, B. *J. Am. Chem. Soc.* **2011**, *133*, 18590. (b) Kline, M. A.; Wei, X. X.; Horner, I. J.; Liu, R.; Chen, S.; Chen, S.; Yung, K. Y.; Yamato, K.; Cai, Z. H.; Bright, F. V.; Zeng, X. C.; Gong, B. *Chem. Sci.* **2015**, *6*, 152.
(10) (a) Parra, R. D.; Zeng, H. Q.; Zhu, J.; Zheng, C.; Zeng, X. C.; Gong, B. *Chem.—Eur. J.* **2001**, *7*, 4352. (b) Parra, R. D.; Gong, B.; Zeng, X. C. *J. Chem. Phys.* **2001**, *115*, 6036. (c) Parra, R. D.; Furukawa, M.; Gong, B.; Zeng, X. C. *J. Chem. Phys.* **2001**, *115*, 6030.
(11) Cabrita, E. J.; Berger, S. *Magn. Reson. Chem.* **2001**, *39*, S142.
(12) (a) Dewar, M. J. S.; Zoebisch, E. G.; Healy, E. F.; Stewart, J. J. P. *J. Am. Chem. Soc.* **1985**, *107*, 3902. (b) Plumley, J. A.; Dannenberg, J. J. *J. Am. Chem. Soc.* **2010**, *132*, 1758. (c) Kozlowska, U.; Maisuradze, G. G.; Liwo, A.; Scheraga, H. A. *J. Comput. Chem.* **2010**, *31*, 1154. (d) Liang, S.; Roitberg, A. E. *J. Chem. Theory Comput.* **2013**, *9*, 4470.
(13) Lipson, H.; Stokes, A. R. *Proc. R. Soc. London, Ser. A* **1942**, *181*, 101.

DOI: 10.1021/jacs.5b02552
J. Am. Chem. Soc. 2015, 137, 5879−5882